Pakistan J. Zool., vol. 55(2), pp 743-753, 2023 DOI: https://dx.doi.org/10.17582/journal.pjz/20200625160645

High Pathogenicity Island (HPI) Main Structural Genes and their Bioinformatics Analysis in Clinically Isolated *E. coli* from Saba Pigs

Chunlan Shan[1], Chaoying Liu[1], Qin Lu[1], Guowen Fu[2], Syed Aftab Hussain Shah[3], Rana Waseem Akhtar[4], Ru Zhao[2], Libo Gao[2], Chang Liu[2], Shushu Miao[2], Hongdan Wang[2] and Hong Gao[2]*

[1]*College of Animal Science and Technology, Yunnan Agricultural University, Kunming, Yunnan, 650201, China*
[2]*College of Veterinary Medicine, Yunnan Agricultural University, Kunming, Yunnan, 650201, China*
[3]*Pakistan Scientific and Technological Information Center, Quaid-i-Azam University Campus, Islamabad, 44000, Pakistan*
[4]*Department of Veterinary and Animal Sciences, Muhammad Nawaz Shareef University of Agriculture, Multan, 66000, Pakistan*

Chunlan Shan, Chaoying Liu and Qin Lu contributed equally to this work.

Article Information
Received 25 June 2020
Revised 18 October 2020
Accepted 10 November 2020
Available online 15 April 2022 (early access)
Published 21 December 2022

Authors' Contribution
CS presented the concept, conducted the research and wrote the first draft. CS and CL planned methodology. QL and SAHS wrote and edited the manuscript. GF and CL worked on software and validation. SAHS managed bibliography. RWA curated data. SM and HW performed formal analysis. RZ and LG provided resources. HG provided research funds and supervised the study.

Key words
***E. coli*, High pathogenicity island, Protein prediction, Pathogenicity, Histopathology**

ABSTRACT

High pathogenicity island (HPI), a critical genomic element of pathogenic *Yersinia*bactin (Ybt) carries out synthesis, regulation, transportation as well as virulence. As a virulent determinant for the *E. coli*, the role of HPI in Saba pig was explored to provide some perspective about disease association. This is the first study in which 44 *E. coli* superior serotype strains were isolated and identified from Yunnan Saba pigs. The genomic DNA of all isolated superior serotypes of *E. coli* was obtained. Five major high pathogenicity island (HPI) structural genes (irp1, irp2, irp3, irp4 and irp5) were cloned, sequenced and referenced with GenBank database. The sequence identities of irp1, irp2, irp3, irp4 and irp5 with GenBank were 98 %, 99 %, 99 %, 98 %, and 99 %, respectively. Forty-four *E. coli* isolates characterized similarity with enteroinvasive *E. coli* (EIEC), uropathogenic *E. coli* (UPEC), Y. pestis and enteropathogenic *E. coli* (EPEC). The secondary and tertiary structures of high molecular weight proteins (HMWPs), encoded by five structural genes, were predicted using bioinformatics tools. These proteins had differences in random curls, α-helix and slight amount of β-sheet. After validation, 10 iron deficient isolates expressed the ferritin HMWPs similar to those of *Yersinia*. Later on, Kunming mice were infected with *E. coli* HPI^+ and HPI^- strains, respectively for the histopathology examination. The higher organ damage was observed by *E. coli* HPI^+ than HPI^- strain in mice. This study postulates the predicted protein structures of major genes, and validates the HMWP expression under iron starvation and provides a theoretical basis for prevention and treatment of *E. coli* related diseases.

INTRODUCTION

Escherichia coli is a typical Gram-negative and coliform bacterium, which is ubiquitously distributed among intestinal tract of warm-blooded animals and the environment (Croxen *et al*., 2013; Stromberg *et al*., 2017). The infections caused by *E. coli* span from the gastrointestinal tract to extra-intestinal sites, such as the urinary tract, bloodstream, and central nervous system (Croxen and Finlay, 2010; Kaper *et al*., 2004). High pathogenicity island (HPI) is one of the specific virulence determinants of

* Corresponding author: gaohongping@163.com
0030-9923/2023/0002-743 $ 9.00/0

Abbreviations

CAS, Chrome azurol S; DIG-dUTP, Digoxigenin- Deoxyuridine triphosphate; Irp, iron regulatory protein; *E. coli, Escherichia coli;* ECOR31, *Escherichia coli* ECOR31; ECOR38, *Escherichia coli* ECOR38; EIEC, Enteroinvasive *Escherichia coli*; EPEC, Enteropathogenic *Escherichia coli*; H-E, Hematoxylin- eosin; HMWPs, High molecular weight proteins; HPI, High pathogenicity island; pI, Isoelectric point; KM, Kunming; Mw, Molecular weight; NBT/BCIP, Nitro blue tetrazolium/ 5-bromo-4-chloro-3-indolyl phosphate; PCR, Polymerase Chain Reaction; IPEC-J2, Porcine small intestine epithelial cells; SDS-PAGE, Sodium dodecyl sulfate–polyacrylamide gel electrophoresis; UPEC, uropathogenic *E. coli;* Ybt, Yersiniabactin.

E. coli, which contributes to synthesis, regulation, and transportation of siderophore yersiniabactin (Ybt) (Magistro *et al*., 2017; Schubert *et al*., 2002). This pathogenicity island was originally described in *Yersinia* spp. with a 35-45 kb genome, and spreads across a variety of Enterobacteriaceae, and is potentially considered virulent (Heesemann *et al*., 1993; Lawlor *et al*., 2007).

HPI has a functional core region, in which the irp2-irp1-irp3-irp4-irp5-FyuA gene axis is termed irp2-FyuA cluster, and irp2 is the marker gene among them (Schouler *et al*., 2012). The irp2-FyuA gene cluster is reported to be closely involved in the synthesis of siderophore *Yersinia* (Buchrieser *et al*., 1999; Gehring *et al*., 1998; Rakin *et al*., 1999; Liu *et al*., 2018). High molecular weight proteins (HMWPs), which are encoded by irp2-FyuA gene cluster and they have members such as HMWP1, 2, 3, 4 and 5, respectively. HMWPs are actively expressed in highly pathogenic *Yersinia* strains and play an important role in the synthesis of *Yersinia* siderophores (Heesemann, 1987; Liu *et al*., 2018). A few *Y. enterocolitica* isolates from chicken and fish are capable to produce HMWPs (Shanmugapriya *et al*., 2014). Further evidence entails that Acyl-CoA hydrolysis, a HMWP1 subunit, could promote a cascade reaction of four acyl-enzyme intermediates during hydrolytic editing (Suo *et al*., 2000). HMWP2, a specific protein which is encoded by irp2 gene of highly pathogenic *Yersinia* species, participates in the non-ribosomal synthesis of small biologically active peptides (Guilvout *et al*., 1993). The pathogenicity of irp2-FyuA gene cluster, encoding the virulence of highly pathogenic *Yersinia* bacteria, has been studied in human (Schubert *et al*., 1998), but the mechanism of its pathogenesis has not been clearly described yet.

Saba pig, is an excellent and indigenous local breed in Yunnan province of China, which is domesticated in a relatively isolated environment and distributed in a high altitude areas (>1500 m above the sea level), (Lian *et al*., 2005). *E. coli* strain has been isolated previously from Saba pig and the sick pigs developed noticeable symptoms such as diarrhea, grayish or yellow loose stools, and emaciation, which are responsible for the high morbidity and mortality of *E. coli*-related diseases and offers challenges to the veterinary community (Lu *et al*., 2014; Wei *et al*., 2018). As a virulent determinant for the *E. coli*, the role of HPI in Saba pig and its characteristic still remains elusive and needs further exploration.

In the present study, 44 *E. coli* superior serotype strains were isolated and identified from Saba pigs. The HPI structural genes of irp1, irp2, irp3, irp4 and irp5 were detected and sequenced. Subsequently the evolutionary tree was drawn and homology was calculated. In the case of iron deficiency, HMWPs were detected in all *E. coli* isolates by sodium dodecyl sulfate–polyacrylamide gel electrophoresis (SDS-PAGE). Furthermore, Kunming (KM) mice were infected with *E. coli* HPI^+ and HPI^- strains, respectively and compared with saline control and the histopathology was carried out. Our data shows the role of HPI in the occurrence of *E. coli* associated diseases in Saba pigs. Moreover, this study may provide interesting perspective that could benefit further research into bacterial response in some native animals.

MATERIALS AND METHODS

Ethics approval

Animals involved in this study were looked after according to the guidelines of Animal Care and Use Committee of Yunnan Agricultural University. All standard procedures concerning animal care and management were taken throughout the experiment.

Experimental strains and animals

Forty-four *E. coli* superior serotype strains were isolated and identified from forty-eight live Yunnan Saba pigs (obtained from a farm in Chuxiong County, Yunnan Province) through fecal and rectal swabs. The sampling was carried out after seeking formal written consent of the farm. *Klebsiella pneumoniae* (ATCC700603), was purchased from China Institute of Veterinary Drug Control (Beijing, China), and was used as the negative control. Avian pathogenic *E. coli* (China Veterinary Culture Collection Center1565; CVCC 1565) was donated by Dr. Jiao XA (Yangzhou University, China), and treated as a positive control. The serotypes were identified as: O3 (19/44), O4 (15/44), O24 (10/44).

Twelve healthy 5-week-old Kunming (KM) mice (female, weight 20-25g) were purchased from Kunming Medical University with prior written consent about their use and were housed in three cages in best management conditions (the animal breeding room at Yunnan Agricultural University) and acclimatized prior to experimentations. All mice were provided feed and water *ad libitum*. Twelve mice were randomly divided into 3 groups (n=4 mice per group): HPI^+-infected group, HPI^--infected group and saline control. Mice were infected by intraperitoneal injection with 0.3 mL of bacterial suspension (3×10^8 cfu/mL). The control group was administered saline by the same way. After treatment of 24 h, all mice were euthanized by cervical dislocation to record gross pathological changes and collect tissue samples.

E. coli *genomic DNA extraction and PCR detection of main structural genes of HPI*

The genomic DNA of all isolated superior serotypes

of *E. coli* from Saba pig was extracted according to manufacturer's instructions (Beijing Bio Teke Co. Ltd., China) and protocol (Sakallah *et al*., 1995). All extracted DNA was stored at -20°C for further use. The GenBank database was referred and the sequences of irp1, irp2, irp3, irp4 and irp5 were blasted to obtain a conserved region. Oligo for each gene was designed by Primer 5.0 software and synthesized by Shuoyang Company (Table I). PCR reaction mixture (50µl) was processed as follows: pre-denaturation at 95°C for 15 min; denaturation at 94°C for 1 min, annealing at 54°C for 1 min, extension at 72°C for 1 min, a total of 32 cycles; extension at 72°C for 10 min, and storage at 4°C. Gel electrophoresis was carried out and photographs were visualized through gel imaging system.

Colony spots in situ hybridization detection of main molecular structures in superior serotype E. coli *HPI*

Colony spots in situ hybridization was carried out according to the protocols (Höltke *et al*., 1995; Southern, 1975). The PCR products were subjected to gel recovery, plasmid transformation, ligation vector, and restriction enzyme digestion. Then DNA was labeled by random primer method and DIG-dUTP (digoxigenin-deoxyuridine triphosphate). Chromogenic substrate NBT/BCIP (nitro blue tetrazolium/ 5-bromo-4-chloro-3-indolyl phosphate) was used for color development of hybrid molecules.

Comparison of HPI homology of superior serotype E. coli

Superior serotype strain samples possessing *HPI irp* (iron regulatory protein)1, *irp2, irp3, irp4* and *irp5* gene, as identified by PCR, were collected for gel recovery (operated according to the specifications of Bioteke's multifunctional DNA purification and recovery kit), and the products were sequenced by Huada Gene Technology Co., Ltd. The results of the sequencing yielded genetic trees by homology comparison and mapping of phylogenetic trees.

Bioinformatics analysis of superior serotype E. coli *HPI*

The secondary structures of protein encoded by *HPI irp1, irp2, irp3, irp4* and *irp5* genes were predicted respectively (http://bioinf.cs.ucl.ac.uk/psipred/). The isoelectric point (pI) and molecular weight (Mw) of proteins, encoded by five genes, were analyzed by using ExPASy's online compute pI/Mw tool. The five gene protein glycosylation sites of HPI were predicted through NetNGlyc 1.0 Server (http://www.cbs.dtu.dk/services/NetNGlyc/).

Using the homology modeling method (http://www.expasy.org/swissmod/ SWISS-MODEL.html), the amino acid sequences of five proteins were submitted to the SWISS-MODEL Server for automatic modeling, and the tertiary (three-dimensional) protein structures were predicted.

Expression of high molecular weight proteins (HMWPs) in superior serotype E. coli *strains*

HMWP1, HMWP2, HMWP3, HMWP4 and HMWP5 in *E. coli* superior serotype HPI strains were detected by SDS-PAGE at a concentration of 0.2 mM 2, 2′-dipyridine iron deficiency. Proteins were extracted after expression of HMWPs, and added appropriate sample buffer and placed in boiling water at 100°C for 5-15 min to denature proteins. After two-dimensional electrophoresis, Coomassie blue was used for staining.

Simple microscopic histopathology

HPI^+ and HPI^- strains of pathogenic *E. coli* were identified and preserved by the Department of Animal

Table I. PCR primers used in this study.

Primer designation	Sequence of primer (5'—3')	Annealing temperature	Length of product(bp)	*GenBank
irp1	CAGCCTCACGGCCCTTAT	54	360	Y12527.1
	CGGCGTATGCTCAGTCAGTA			
irp2	TTCCTTCAGCATCGCCTGTTA	55	484	L18881.1
	CAAGCCCGACATACTCAATCT			
irp3	TGCTGCTATTGGGTAAACACG	53	407	Y12527.1
	GCGACAAACAGGCTGGATGA			
irp4	CGAACTGGAAGCGTCCGTAT	67	459	Y12527.1
	TCGCCGTCAATCACCACC			
irp5	CCCTGCTGTTCGCCTTGT	57	786	Y12527.1
	CCTGGCTGTGGAGAATAGTGG			

*Reference: *Yersinia enterocolitica* HMWP1 (irp1), HMWP3 (irp3), HMWP4 (irp4) and HMWP5 (irp5) genes. GenBank, Y12527.1; (https://www.ncbi.nlm.nih.gov/nuccore/Y12527); *Reference, *Yersinia enterocolitica* HMWP2 (irp2) gene, complete cds. GenBank, L18881.1; (https://www.ncbi.nlm.nih.gov/nuccore/L18881).

Pathology (Yunnan Agricultural University, China) (Liu *et al*., 2018). HPI^{+} and HPI^{-} strains have the same serotype (O119) and biochemical characteristics which were tested by the method (Linxi *et al*., 2019). The liver and kidney were sampled from each group (HPI^{+}-infected group, HPI^{-}- infected group and saline control) and fixed with 10% formalin, embedded in paraffin, cut into 6 μm thick sections with a sledge microtome (Leica RM 2235, Germany), and stained using the hematoxylin- eosin (H-E) method. These sections were observed under 40 × /100 × /400 × amplifications (Olympus CX43 microscope, Japan).

Ultrastructural histopathology

The liver and kidney were sampled from each group (HPI^{+}-infected group, HPI^{-}- infected group and saline control) and excised (0.6 cm) immediately and fixed by immersion in 2.5 % buffered glutaraldehyde for more than 4h. Samples were then rinsed in 0.1 M phosphoric acid rinsing solution and post fixed in 1 % osmium tetroxide, dehydrated in ascending grades of ethanol, and embedded in epon, sectioned by ultra-thin slicer (LKBV). The ultra structural changes were observed under transmission electron microscope (TEM-100 CXII, JEOL, Japan) after 3 % uranyl acetate and lead citrate staining.

RESULTS

Major structural genes of HPI in superior serotype strains

PCR and colony spots in situ hybridization were used to detect the presence of *irp1, irp2 irp3, irp4* and *irp5* genes in 44 superior serotypes of *E. coli* strains. The results are shown in Figure 1A-E and Table II. The PCR results were consistent with the expected product size that indicated all *E. coli* isolates carrying *HPI* genes. With colony spots in situ hybridization test, the results were consistent with PCR amplification (Fig. 1F and Table II).

Homology comparison and phylogenetic tree construction of HPI main structural genes

The targeted *HPI* structural genes were sequenced and processed subsequently by DNASTAR software and compared with its "published" sequences in GenBank database. The results are shown in (Fig. 2). The sequence identities of *irp1, irp2, irp3, irp4* and *irp5* with GenBank were 98 %, 99 %, 99 %, 98 %, and 99 %, respectively. The *irp1* gene of isolated strain was closely related to the strain CFT0734 (uropathogenic *Escherichia coli* (UPEC), GenBank). The *irp2* gene was closely related to ECOR38 (*Escherichia coli* ECOR38, B1 group pathogenic, GenBank). The *irp3* gene was closely related to strain D106004 (*Yersinia pestis*, GenBank). The *irp4* gene was closely related to UT189 strain (UPEC, GenBank). The *irp5* gene was closely related to LF82, (enteroinvasive *Escherichia coli* (*EIEC*), GenBank.

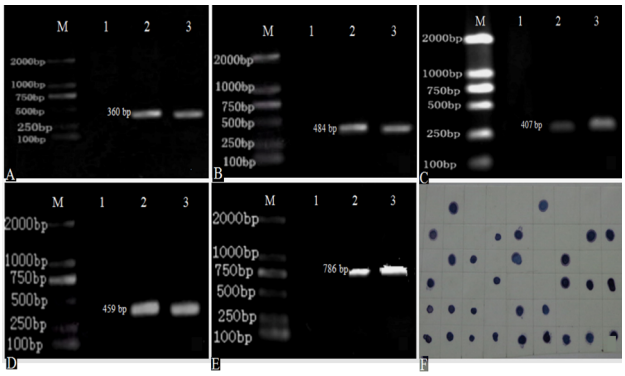

Fig. 1. Detection of PCR and colony spots in situ hybridization for *HPI irp1, irp2, irp3, irp4, irp5* gene (A-E, genetic test results of *HPI irp1, irp2, irp3, irp4, irp5* in turn; F, colony spot hybridization for *irp2* gene; M, DL 2000 Marker; 1, negative control; 2, positive strain; 3, experimental strain).

Table II. Detection of *HPI irp1, irp2, irp3, irp4* and *irp5* genes in all 44 *E. coli* isolates from Saba pigs.

Virulence gene	Positive number stain	Positive rate (%)	Superior serotype positivestain		
			O_3	O_4	O_{24}
irp1	38	86.37%	17	12	9
irp2	39	88.64%	18	12	9
irp3	26	59.09%	9	6	8
irp4	30	68.18%	13	11	6
irp5	33	75.00%	16	8	9

Irp, iron regulatory protein.

Prediction of secondary and tertiary protein structure encoded by HPI irp1, irp2, irp3, irp4 *and* irp5 *genes and expression of HMWP proteins in HPI experimental strains*

The data on secondary structure prediction of proteins that were encoded by *HPI irp1, irp2, irp3, irp4* and *irp5* genes, pI, MW and protein glycosylation sites is shown in Figure 3 and Table III. The three-dimensional structures of HPI irp1, irp2, irp3, irp4 and irp5 proteins are shown in Figure 4. The structures of the five proteins are consistent with the prediction of the secondary structure, which is a mixture of α-helix, β-sheet and random coil. The synthesis of iron vector of *E. coli* dominant serotype HPI strain was detected by chrome azurol S (CAS) solid medium. Under iron deficiency conditions, 10 strains of *E. coli* dominant serotype HPI expressed five high molecular weight proteins comprising

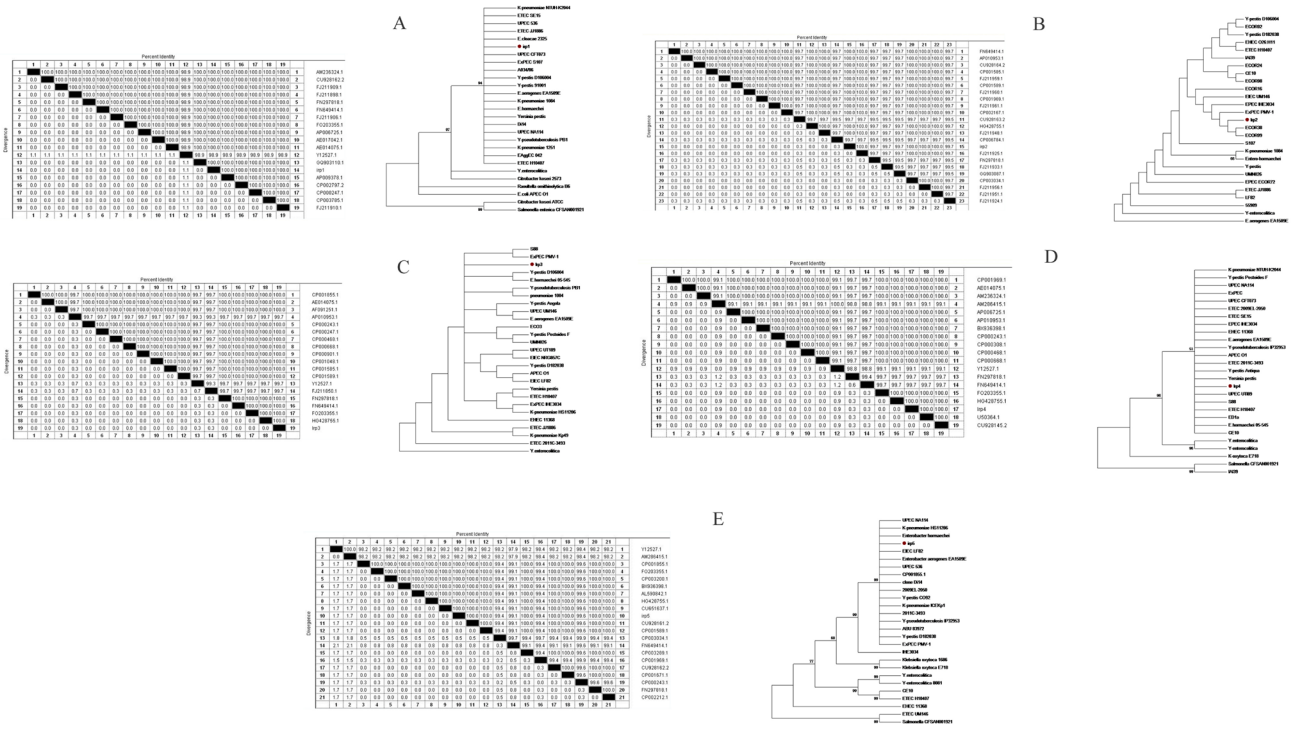

Fig. 2. The homology of HPI major part gene sequences and phylogenetic trees (A-E, in sequence, the homology comparison of *HPI irp1, irp2, irp3, irp4,* and *irp5* part gene sequence and corresponding phylogenetic trees).

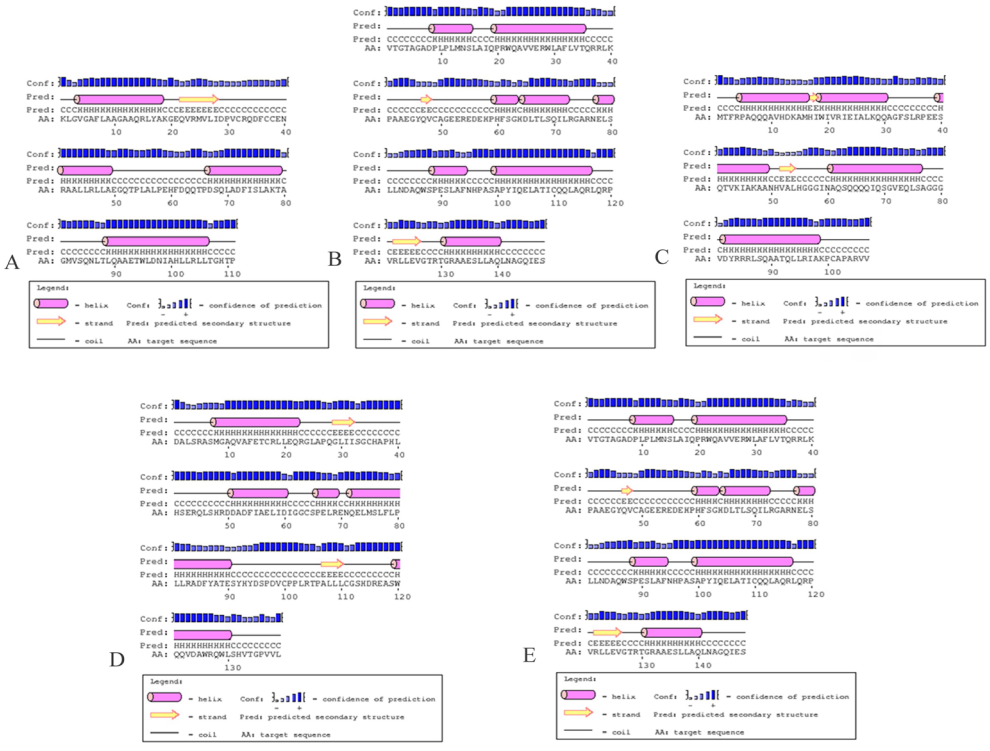

Fig. 3. Predication of protein secondary structure of HPI major structure genes (A-E, in sequence, prediction of protein secondary structure of *irp1, irp2, irp3, irp4* and *rp5* genes, respectively).

HMWP1, HMWP2, HMWP3, HMWP4 and HMWP5, while the other 15 strains expressed different proteins from HMWPs (Fig. 5). The HPI major structural protein genes showed that 5 types of proteins mainly include more random curls, α-helix and slight amount of β-sheet; among which the random coils accounted for a larger proportion. Analysis of isoelectric point verified that irp1, irp2, irp4 and irp5 were acidic proteins, while irp3 was the basic protein. Subsequent SDS-PAGE electrophoresis (pH 8.8) did not detect irp3 protein bands.

Table III. Prediction of secondary structures of five major structural genes in all 44 *E. coli* isolates from Saba pigs.

Variables	*irp1*	*irp2*	*irp3*	*irp4*	*irp5*
The number of spiral	55	81	67	59	67
Extended chain	7	7	5	8	5
Swiss roll	39	60	35	72	35
pI	5.85	5.79	10.57	5.05	5.13
Mw (Da)	12068.93	16344.48	11661.4	15534.54	26713.50
Glycosylation site	1	0	0	0	0

pI, Isoelectric point; Mw, molecular weight.

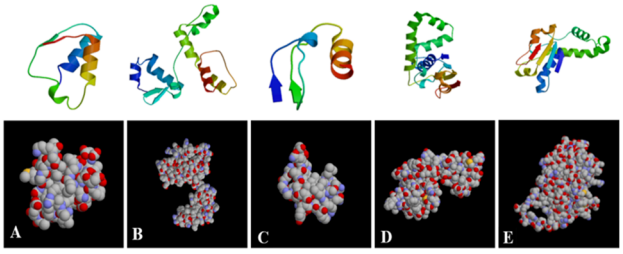

Fig. 4. Prediction of protein tertiary structure of HPI major structure genes (A-E, in sequence, prediction of protein tertiary structure prediction of *irp1, irp2, irp3, irp4* and *irp5* genes).

Simple microscopic histopathological observations

As shown in Figure 6, gross pathological findings showed severe hemorrhage and swelling in the lungs and liver. There was mild bleeding in the renal cortex. The wall of small intestine was bleeding and thinning, which filled with yellow contents (Fig. 6). No visible microscopic lesions were observed in the liver and kidney control groups (Fig. 7A, D). The hepatocyte enlargement and disordered arrangement of hepatocyte cords was observed. Moreover, some lymphocyte infiltrations were seen in the hepatic sinus and few red blood cells were observed in the interlobular veins in the portal area (Fig. 7B, C). The glomerulus was enlarged and filled the entire renal cavity. The epithelial cells of the renal tubules were blurred and shed. A few red blood cells were also observed in the renal stroma, and local inflammatory cells were infiltrated (Fig. 7E, F). In addition, more severe histopathological changes were observed in the HPI^+ -infected group compared to HPI^-infected group.

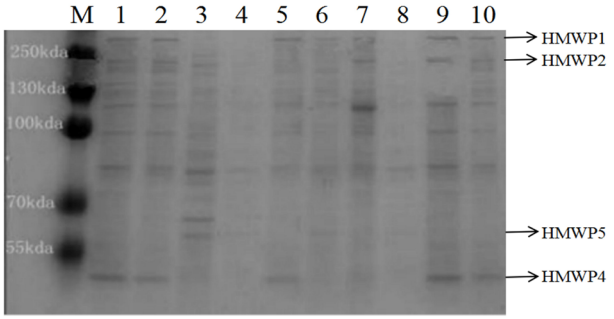

Fig. 5. The expression profile of HMWPs under iron starvation (M: Protein marker; 1, Positive strain; 2-10, The experimental strains. HMWPs bands, irp1-348kDa, irp2-229kDa, irp4-29kDa, irp5-57kDa; irp3 was the basic protein (pH 8.8) so did not detect protein bands).

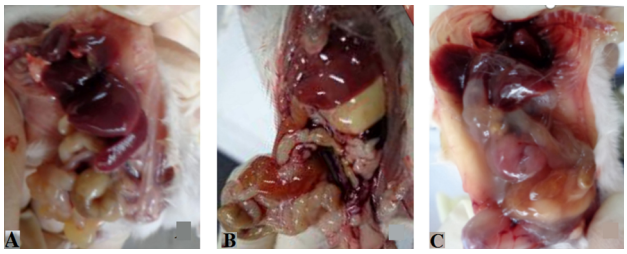

Fig. 6. Gross pathological signs of mice (A, control group; B, HPI^+ infection group; C, HPI^- infection group).

Ultra structural histopathological observations

Under the transmission electron microscope, the liver cells of the control mice had round nucleus, clear nuclear membrane, obvious nucleolus, and often chromatin was evenly distributed in the nucleus; the mitochondria and endoplasmic reticulum around the nucleus were abundant, and the round rod-shaped or spherical, mitochondrial crest structure is clear, rough endoplasmic reticulum (RER) is relatively developed, neatly arranged, and abundant ribosomal particles are distributed on it, without ribosome shedding and lipidation. After infection in HPI mice, the complete morphology of liver cells disappeared, the nucleus was irregular, the nuclear membrane was uneven, and the nuclear pores were significantly increased;

the mitochondria were deformed and the ridges were disordered; the rough endoplasmic reticulum was swollen, and the ribosomal particles were reduced with visible lipidation. The HPI + was more severe than the HPI- group.

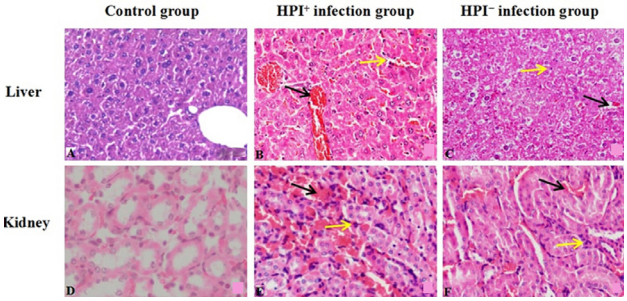

Fig. 7. Histopathology observations of liver and kidney in mice (HE, 400×); A, liver of control group; B, liver of HPI$^+$-infection group; C, liver of HPI$^-$-infection group; D, kidney of control group; E, kidney of HPI$^+$-infection group; F, kidney of HPI$^-$-infection group). Black arrow indicates red blood cells; yellow arrow indicates lymphocyte infiltrations.

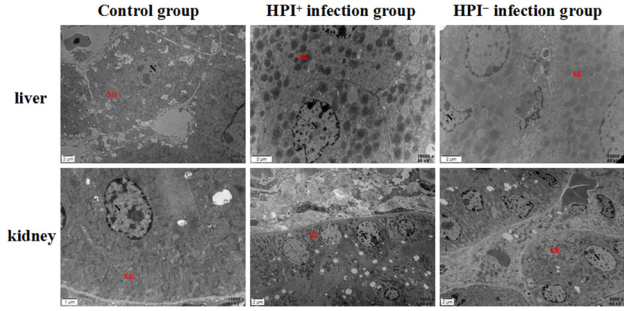

Fig. 8. Ultrastructural histopathology observations of liver and kidney in mice. Control group, HPI$^+$-infection group, and HPI$^-$-infection group.

Under the transmission electron microscope, the kidney cells of the control group mice have a clear structure of renal tubular epithelial cells with large and round nuclei, often chromatin is evenly distributed in the nucleus; the inner fold of the plasma membrane at the base and the structure of the tubular basement membrane are complete; the mitochondrial ridge structure is clear and densely arranged; the microvilli are densely arranged in the lumen, and the tight connection between the cells is clearly visible. After infection in HPI group mice, most of the renal tubular epithelial cells show shrunken nucleus with abnormally rich heterochromatin condensation; and a small amount of nucleoli dissolves; the microvilli on the cell surface are sparsely arranged; the base is swollen, and the inner pleats disappear; mitochondrial swelling, mitochondrial crest structure is fuzzy, and some crests are broken; rough endoplasmic reticulum ribosomes reduce; a large number of lipid droplets can be seen. The HPI + was more severe than the HPI- group (Fig. 8).

DISCUSSION

Major structural genes of HPI in superior serotype strains

The current study found that PCR results were consistent with the expected product size that indicated all *E. coli* isolates carrying *HPI genes*. With colony spots in situ hybridization test, the results were consistent with PCR amplification. HPIs, a subset of genomic islands, encode several virulent determinants such as toxins and siderophore systems and play a key role in the evolution of pathogenic bacteria such as *E. coli* (Hu *et al*., 1998; Poey and Lavina, 2018; Schneider *et al*., 2011). A possible mechanism revealed that HPIs, among *E. coli* (ECOR31) and other Enterobacteriaceae, more likely caused the extra-intestinal infections due to possessing an additional 35 kb fragment at the right border compared to traditional HPIs in *E. coli* and *Yersinia* species (Schubert *et al*., 2004).

Homology comparison and phylogenetic tree construction

In the present study, the sequence identities of irp1, irp2, irp3, irp4 and irp5 with GenBank were 98%, 99%, 99%, 98%, and 99%, respectively. The *irp1* gene of isolated strain was closely related to the strain CFT0734 (uropathogenic *Escherichia coli* (UPEC), GenBank). The *irp2* gene was closely related to ECOR38 (*Escherichia coli* ECOR38, B1 group pathogenic, GenBank). The *irp3* gene was closely related to strain D106004 (*Yersinia pestis*, GenBank). The *irp4* gene was closely related to UT189 strain (UPEC, GenBank). The *irp5* gene was closely related to LF82, (enteroinvasive *Escherichia coli* (*EIEC*), GenBank). In contrast to our study, overall, irp1 and irp2 were present in 63 and 77% of *E. coli* strains, respectively, and fyuA was detected in 77% of isolates (Koczura and Kaznowski, 2003). The sizes of PCR products generally reckoned with expected values except four isolates (RK12, RK13, RK18 and RK22) which represented a 750bp product of fyuA (Koczura and Kaznowski, 2003) that was shorter than the corresponding fragment in *Yersinia* pestis (780bp long); in our study, the sizes of PCR products of five structural genes, i.e., *irp1, irp2, irp3, irp4* and *irp5* were 360, 484, 407, 459, 786bp, respectively and these were referenced to *Yersinia enterocolitica* (GenBank: Y12527.1 and GenBank: L18881.1). Furthermore, the identities between *Yersinia enterocolitica* (Yen; O:8 WA strain) HPI and avian pathogenic *E. coli HPI irpl* (799bp), *irp2* (414bp), *irp3* (798bp), *irp4* (504bp), *irp5* (758bp) and *fyuA* (948bp) were found to be 98 %, 98 %, 98 %, 95 %, 98

%, and 98%, respectively (Xu *et al*., 2010). This highlights that high HPI expression implies widespread occurrence and greater pathogenicity and vice versa. The variation in number of *E. coli* strains, their expression and virulence may also be related to the type of species as well sampling site. The sampling source of *E. coli* (44 strains) was fecal and rectal swabs from live Yunnan Saba pigs in our study whereas 35 strains *of E. coli* were clinical specimens comprising of urine (18), blood (5), cervical canal (3), semen (3), conjunctiva (2), wound (2), foreskin abscess (1), and cerebrospinal fluid (1) (Koczura and Kaznowski, 2003). The results further suggest that as *E. coli* strains of Yunnan Saba pigs carry genes which are located on the *Yersinia enterocolitica* HPI, which may provide a chance of transferring these genes between *Yersinia enterocolitica* and *E. coli* strains of Yunnan Saba pigs.

Prediction of secondary and tertiary protein structure

The structures of the five proteins were consistent with the prediction of the secondary structure, which are mixture of α-helix, β-sheet and random coil. Under iron deficiency conditions, 10 strains of *E. coli* dominant serotype HPI expressed five high molecular weight proteins comprising HMWP1, HMWP2, HMWP3, HMWP4 and HMWP5, while the other 15 strains expressed different proteins from HMWPs. With a fast increasing pool of identified tertiary structures, the significance of protein structure comparison corresponds to that of sequence alignment (Holm and Sander, 1993). The HPI major structural protein genes showed that 5 types of proteins mainly include more random curls, α-helix and slight amount of β-sheet; among which the random coils accounted for a larger proportion. Since the epitopes easily form secondary structures especially by random coils, this indicates that these five proteins are rich in antigenic epitopes. The random curly structures are comparatively prominent, mainly on the surface of the protein molecules, and often contain advantageous antigen epitope (Liu *et al*., 2007), so it is easy to induce the host to produce effective immune response. Analysis of isoelectric point verified that irp1, irp2, irp4 and irp5 were acidic proteins, while irp3 was the basic protein. Subsequent SDS-PAGE electrophoresis (pH 8.8) did not detect irp3 protein bands. Many pathogens uptake iron with some low molecular weight high iron chelates -siderophores, which are transported into bacterial cells to maintain growth. Siderophore includes element of Enterobacter, *Yersinia* pestis and Bacillus; each of which possess the specific affinity for iron. Its biosynthesis is regulated by concentration of external iron that absorbs iron chelated on the siderophore into cell via a specific cell membrane receptor to meet ferric demand for its growth. HMWPs play an important role in synthesis of siderophore of *Yersinia* bacterium. HMWPs may be involved in the synthesis of siderophore to induce expression of tyrosine receptors and siderophore (Fetherston *et al*., 1995; Johnson and Stell, 2000). When ions are deficient, irp1 and irp2 express HMWP1 and HMWP2, but their sizes are not consistent as molecular weight of HMWP1 and HMWP2 in Yale's plague bacteria were reported as 240 kDa and 228 kDa, respectively (Fetherston *et al*., 1995, 1996) whereas in enterocolitis Yale sen bacteria these were 380 kDa and 228 kDa (Carniel *et al*., 1987, 1996; Pelludat *et al*., 1998). This highlights that HMWP1 stripe size is different, which may be related to glycosylation sites in HMWP1 of the protein prediction. This further implies that the *E. coli* serotype strains containing the HPI may not have expression of HMWPs protein, and additionally, variable protein expression of HMWPs was observed in these *E. coli* serotype HPI strains. A study further reported that not all *E. coli* strains containing HPI could express HMWPs, which may be related to microbe in different living environment and modify the exogenous genes according to their own needs, as well as the extent of iron uptake (Sun *et al*., 2007). The protein prediction of HPI of the superior serotype *E. coli* strain in this study showed the difference of HMWPs protein expression possibly due to the variations in spiral, folding and curly construction in the secondary structure. This expression may also be caused by missing or point mutation in a gene and the strains of serotype and protein expression differences in *E. coli* HPI.

Histopathology

Gross pathological findings and severe hemorrhage and swelling in the lungs and liver were noticed. No visible microscopic lesions were observed in the liver and kidney control groups. In addition, more severe histopathological changes were observed in the HPI^{+} -infected group compared to HPI^{-}infected group. As iron acquisition determinant, HPI is absolutely necessary for expression of the trait of virulence in mice (Carniel *et al*., 1992; Fetherston *et al*., 1992). A study reported that *E. coli* HPI up regulated the expression of IκB-α and IL-1 into porcine small intestine epithelial cells (IPEC-J2), and HPI^{+}-infection strongly induced IL-1 expression than that of HPI^{-}strain (Liu *et al*., 2018). *E. coli* harboring HPI was more virulent in ducklings than that *E. coli* strains without HPI even their genotype was highly homologous (Dian-hong and Xiu-rong, 2011). Transmission electron microscopy also revealed normal histology in control kidney and liver groups; however, HPI^{+} was more drastic than the HPI^{-} group. Our results indicate that the dominant serotype *E. coli* strain containing HPI was more virulent and had certain pathogenic ability.

CONCLUSIONS

This is the first study about *E. coli* HPI structural genes (*irp1, irp2, irp3, irp4* and *rp5*) and their bioinformatics analysis in clinical isolates of Saba pigs. We further postulated the predicted secondary and tertiary protein structures of these major genes, and validated the HMWP expression under iron starvation. In addition, the *E. coli* isolates harboring HPI element induced severe tissue damages in mice than those of HPI-deficiency strains. Our data may provide a new perspective of *E. coli* epidemic and its related diseases in Saba pigs and other animals in future.

ACKNOWLEDGEMENTS

We are grateful to all staff members of College of Animal Science and Technology of Yunnan Agricultural University for their assistance during the experimental work. The funding for conducting this research, analysis and publication was provided by the National Natural Science Foundation of China (Grant No. 31660704 and 31960692).

Statement of conflict of interest

The authors have declared no conflict of interest.

Ethical approval

The research was conducted according to the prevalent ethical standards and guidelines of Animal Care and Use Committee of Yunnan Agricultural University and details have been provided in Methods section.

Availability of data and material

The data supporting this manuscript have already been included and the corresponding author will respond to any query if any.

REFERENCES

Buchrieser, C., Rusniok, C., Frangeul, L., Couve, E., Billault, A., Kunst, F., Carniel, E. and Glaser, P., 1999. The 102-kilobase pgm locus of *Yersinia pestis*: Sequence analysis and comparison of selected regions among different *Yersinia* pestis and *Yersinia* pseudotuberculosis strains. *Infect. Immun.,* **67**: 4851-4861. https://doi.org/10.1128/IAI.67.9.4851-4861.1999

Carniel, E., Guilvout, I. and Prentice, M., 1996. Characterization of a large chromosomal high-pathogenicity island in biotype 1B *Yersinia enterocolitica*. *J. Bact.,* **178**: 6743-6751. https://doi.org/10.1128/JB.178.23.6743-6751.1996

Carniel, E., Guiyoule, A., Guilvout, I. and Mercereau-Puijalon, O., 1992. Molecular cloning, iron-regulation and mutagenesis of the *irp2* gene encoding HMWP2, a protein specific for the highly pathogenic *Yersinia*. *Mol. Microbiol.,* **6**: 379-388. https://doi.org/10.1111/j.1365-2958.1992.tb01481.x

Carniel, E., Mazigh, D. and Mollaret, H.H., 1987. Expression of iron-regulated proteins in *Yersinia* species and their relation to virulence. *Infect. Immun.,* **55**: 277-280. https://doi.org/10.1128/IAI.55.1.277-280.1987

Croxen, M.A. and Finlay, B.B., 2010. Molecular mechanisms of *Escherichia coli* pathogenicity. *Nat. Rev. Microbiol.,* **8**: 26-38. https://doi.org/10.1038/nrmicro2265

Croxen, M.A., Law, R.J., Scholz, R., Keeney, K.M., Wlodarska, M. and Finlay, B.B., 2013. Recent advances in understanding enteric pathogenic *Escherichia coli*. *Clin. Microbiol. Rev.,* **26**: 822-880. https://doi.org/10.1128/CMR.00022-13

Dian-hong, L. and Xiu-rong, Z., 2011. Drug resistance and pathogenicity to ducks of *E. coli* strains with *Yersinia* HPI. *Prog. Vet. Med.,* **1**: Pages?

Fetherston, J.D., Bearden, S.W. and Perry, R.D., 1996. YbtA, an AraC-type regulator of the *Yersinia pestis* pesticin/*Yersinia* bactin receptor. *Mol. Microbiol.,* **22**: 315-325. https://doi.org/10.1046/j.1365-2958.1996.00118.x

Fetherston, J.D., Lillard, J. and Perry, R.D., 1995. Analysis of the pesticin receptor from *Yersinia pestis*: Role in iron-deficient growth and possible regulation by its siderophore. *J. Bact.,* **177**: 1824-1833. https://doi.org/10.1128/JB.177.7.1824-1833.1995

Fetherston, J.D., Schuetze, P. and Perry, R.D., 1992. Loss of the pigmentation phenotype in *Yersinia pestis* is due to the spontaneous deletion of 102 kb of chromosomal DNA which is flanked by a repetitive element. *Mol. Microbiol.,* **6**: 2693-2704. https://doi.org/10.1111/j.1365-2958.1992.tb01446.x

Gehring, A.M., DeMoll, E., Fetherston, J.D., Mori, I., Mayhew, G.F., Blattner, F.R., Walsh, C.T. and Perry, R.D., 1998. Iron acquisition in plague: modular logic in enzymatic biogenesis of *Yersinia*bactin by *Yersinia pestis*. *Chem. Biol.,* **5**: 573-586. https://doi.org/10.1016/S1074-5521(98)90115-6

Guilvout, I., Mercereau-Puijalon, O., Bonnefoy, S., Pugsley, A. and Carniel, E., 1993. High-molecular-weight protein 2 of *Yersinia enterocolitica* is homologous to AngR of *Vibrio anguillarum*

and belongs to a family of proteins involved in nonribosomal peptide synthesis. *J. Bact.,* **175**: 5488-5504. https://doi.org/10.1128/JB.175.17.5488-5504.1993

Heesemann, J., 1987. Chromosomal-encoded siderophores are required for mouse virulence of enteropathogenic *Yersinia* species. *FEMS Microbiol. Lett.,* **48**: 229-233. https://doi.org/10.1111/j.1574-6968.1987.tb02547.x

Heesemann, J., Hantke, K., Vocke, T., Saken, E., Rakin, A., Stojiljkovic, I. and Berner, R., 1993. Virulence of *Yersinia enterocolitica* is closely associated with siderophore production, expression of an iron-repressible outer membrane polypeptide of 65 000 Da and pesticin sensitivity. *Mol. Microbiol.,* **8**: 397-408. https://doi.org/10.1111/j.1365-2958.1993.tb01583.x

Holm, L. and Sander, C., 1993. Protein structure comparison by alignment of distance matrices. *J. mol. Biol.,* **233**: 123-138. https://doi.org/10.1006/jmbi.1993.1489

Höltke, H., Ankenbauer, W., Mühlegger, K., Rein, R., Sagner, G., Seibl, R. and Walter, T., 1995. The digoxigenin (DIG) system for non-radioactive labelling and detection of nucleic acids. An overview. *Cell. mol. Biol. (Noisy-le-Grand, France),* **41**: 883-905.

Hu, W., Lian, L., Su, B. and Zhang, Y., 1998. Genetic diversity of Yunnan local pig breeds inferred from blood protein electrophoresis. *Biochem. Genet.,* **36**: 207-212. https://doi.org/10.1023/A:1018772824353

Johnson, J.R. and Stell, A.L., 2000. Extended virulence genotypes of *Escherichia coli* strains from patients with urosepsis in relation to phylogeny and host compromise. *J. Infect. Dis.,* **181**: 261-272. https://doi.org/10.1086/315217

Kaper, J.B., Nataro, J.P. and Mobley, H.L., 2004. Pathogenic *Escherichia coli*. *Nat. Rev. Microbiol.,* **2**: 123-140. https://doi.org/10.1038/nrmicro818

Koczura, R. and Kaznowski, A., 2003. The *Yersinia* high-pathogenicity island and iron-uptake systems in clinical isolates of *Escherichia coli*. *J. med. Microbiol.,* **52**: 637-642. https://doi.org/10.1099/jmm.0.05219-0

Lawlor, M.S., O'Connor, C. and Miller, V.L., 2007. *Yersinia*bactin is a virulence factor for *Klebsiella pneumoniae* during pulmonary infection. *Infect. Immun.,* **75**: 1463-1472. https://doi.org/10.1128/IAI.00372-06

Lian, L.S., Yan, D.W., Wang, H.Y., Hu, W.P., Lu, S.X., Zhao, S.B. and Li, H.W., 2005. Yunnan local pig species series 2: Saba pig. *Anim. Sci. Vet. Med.,* **22**: 72-74.

Linxi, J., Feilong, G., Chunlan, S., Chaoying, L., Shiyu, W., Yulin, Y. and Hong, G., 2019. Investigation of HPI gene and drug resistance analysis of piglets *Escherichia coli* in large-scale pig farms in Chuxiong, Yunnan province. *China Anim. Husb. Vet. Med.,* **46**: 1849-1855.

Liu, A.-D., Yang, Y., Li, F.-H., Lu, M.-J., Gong, F.-L. and Yang, D.-L., 2007. The prediction of B cell epitopes and HLA estricted CTL epitopes of human cervical cancer oncogene protein. *J. Fourth Milit. Med. Univ.,* **28**: 1260-1263.

Liu, C., Shan, C., Dong, Q., Fu, G., Zhao, R., Yan, Y. and Gao, H., 2018. Pathogenic *E. coli* HPI upregulate the expression of inflammatory factors in porcine small intestinal epithelial cells by ubiquitin proteasome pathway. *Res. Vet. Sci.,* **120**: 41-46. https://doi.org/10.1016/j.rvsc.2018.08.009

Lu, Q., Gao, H., Yan, Y.L., Zhao, R., Cui, Y.Y., Li, X.F., Shao, Z.Y. and Zang, Y.T., 2014. Serotype identification and drug susceptibility testing of Escherichia coli and the detection of the *HPI irp2* gene in Saba pigs. *Heilongjiang Anim. Sci. Vet. Med.,* **2**: 115-117.

Magistro, G., Magistro, C., Stief, C.G. and Schubert, S., 2017. The high-pathogenicity island (HPI) promotes flagellum-mediated motility in extraintestinal pathogenic *Escherichia coli*. *PLoS One,* **12**. https://doi.org/10.1371/journal.pone.0183950

Pelludat, C., Rakin, A., Jacobi, C., Schubert, S. and Heesemann, J., 1998. The *Yersinia* bactin biosynthetic gene cluster of *Yersinia enterocolitica*: organization and siderophore-dependent regulation. *J. Bact.,* **180**: 538-546. https://doi.org/10.1128/JB.180.3.538-546.1998

Poey, M.E. and Lavina, M., 2018. Horizontal transfer of class 1 integrons from uropathogenic *Escherichia coli* to *E. coli* K12. *Microb. Pathogen.,* **117**: 16-22. https://doi.org/10.1016/j.micpath.2018.02.006

Rakin, A., Noelting, C., Schubert, S. and Heesemann, J., 1999. Common and specific characteristics of the high-pathogenicity island of *Yersinia enterocolitica*. *Infect. Immun.,* **67**: 5265-5274. https://doi.org/10.1128/IAI.67.10.5265-5274.1999

Sakallah, S.A., Lanning, R.W. and Cooper, D.L., 1995. DNA fingerprinting of crude bacterial lysates using degenerate RAPD primers. *Genome Res.,* **4**: 265-268. https://doi.org/10.1101/gr.4.5.265

Schneider, G., Dobrindt, U., Middendorf, B., Hochhut, B., Szijártó, V., Emody, L. and Hacker, J., 2011. Mobilisation and remobilisation of a large

archetypal pathogenicity island of uropathogenic Escherichia coli *in vitro* support the role of conjugation for horizontal transfer of genomic islands. *BMC Microbiol.,* **11**: 210. https://doi.org/10.1186/1471-2180-11-210

Schouler, C., Schaeffer, B., Brée, A., Mora, A., Dahbi, G., Biet, F., Oswald, E., Mainil, J., Blanco, J. and Moulin-Schouleur, M., 2012. Diagnostic strategy for identifying avian pathogenic *Escherichia coli* based on four patterns of virulence genes. *J. clin. Microbiol.,* **50**: 1673-1678. https://doi.org/10.1128/JCM.05057-11

Schubert, S., Dufke, S., Sorsa, J. and Heesemann, J., 2004. A novel integrative and conjugative element (ICE) of *Escherichia coli*: the putative progenitor of the *Yersinia* high-pathogenicity island. *Mol. Microbiol.,* **51**: 837-848. https://doi.org/10.1046/j.1365-2958.2003.03870.x

Schubert, S., Picard, B., Gouriou, S., Heesemann, J. and Denamur, E., 2002. *Yersinia* high-pathogenicity island contributes to virulence in *Escherichia coli* causing extraintestinal infections. *Infect. Immunol.,* **70**: 5335-5337. https://doi.org/10.1128/IAI.70.9.5335-5337.2002

Schubert, S., Rakin, A., Karch, H., Carniel, E. and Heesemann, J., 1998. Prevalence of the "high-Pathogenicity Island" of *Yersinia* species among *Escherichia coli* strains that are pathogenic to humans. *Infect. Immunol.,* **66**: 480-485. https://doi.org/10.1128/IAI.66.2.480-485.1998

Shanmugapriya, S., Senthilmurugan, T. and Thayumanavan, T., 2014. Genetic diversity among *Yersinia enterocolitica* isolated from chicken and fish in and around Coimbatore city, India. *Iran. J. Publ. Hlth.,* **43**: 835.

Southern, E.M., 1975. Detection of specific sequences among DNA fragments separated by gel electrophoresis. *J. mol. Biol.,* **98**: 503-517. https://doi.org/10.1016/S0022-2836(75)80083-0

Stromberg, Z.R., Johnson, J.R., Fairbrother, J.M., Kilbourne, J., Van Goor, A., Curtiss, R. and Mellata, M., 2017. Evaluation of *Escherichia coli* isolates from healthy chickens to determine their potential risk to poultry and human health. *PLoS One,* **12**. https://doi.org/10.1371/journal.pone.0180599

Sun, S.X., Chen, S.Q., Wang, Y. and Luo, H.J., 2007. Structure and function of high pathogenicity island of *Yersinia enterocolitica* WA in enteroaggregative *E. coli*. *Zhongguo Zuzhi Gongcheng Yanjiu yu Linchuang Kangfu,* **11**: 5777-5779.

Suo, Z., Chen, H. and Walsh, C.T., 2000. Acyl-CoA hydrolysis by the high molecular weight protein 1 subunit of *Yersinia*bactin synthetase: Mutational evidence for a cascade of four acyl-enzyme intermediates during hydrolytic editing. *Proc. natl. Acad. Sci.,* **97**: 14188-14193. https://doi.org/10.1073/pnas.260495697

Wei, H., Li, J.J. and Wang, W.H., 2018. Causes, prevention and control measures of swine coli bacillosis. *Shaanxi J. agric. Sci.,* **64**: 92-95.

Xu, L., Qi, K.-Z. and Peng, K.-S., 2010. Detection of the core area located on *Yersinia* high pathogenicity island in the avian pathogenic *Escherichia coli* strain (CVCC1565). *J. Biol.,* **27**: 49-50.